

AGN evolution from large and deep X-ray surveys

Marcella Brusa¹

¹max Planck Institute für Extraterrestrische Physik,
 Giessenbachstrasse, 1 DE-85748, Garching bei München, Germany
 email: marcella@mpe.mpg.de

Abstract. Over the last few years, the existence of mutual feedback effects between accreting supermassive black holes powering AGN and star formation in their host galaxies has become evident. This means that the formation and the evolution of AGN and galaxies should be considered as one and the same problem. As a consequence, the search for, and the characterization of the evolutive and physical properties of AGN over a large redshift interval is a key topic of present research in the field of observational cosmology. Significant advances have been obtained in the last ten years thanks to the sizable number of XMM-Newton and Chandra surveys, complemented by multiwavelength follow-up programs. I will present some of the recent results and the ongoing efforts (mostly from the COSMOS and CDFS surveys) aimed at obtaining a complete census of accreting Black Holes in the Universe, and a characterization of the host galaxies properties.

Keywords. galaxies:active, galaxies:starburst, X-rays:galaxies

Since the launch in 1999 of both the XMM-Newton and Chandra satellites, a large (> 30) number of surveys covering a wide fraction of the area vs. depth plane (see Fig. 1 in Brandt & Hasinger 2005 see also Hickox 2009) have been performed and our understanding of AGN properties and evolution has received a major boost. Thanks to vigorous programs of multiwavelength follow-up campaigns which, since a few years, have become customary, sensitive X-ray observations turned out to be highly efficient in unveiling weak and/or elusive accreting black holes, in a variety of otherwise *non-active* galaxies, such as (among others): X-ray Bright Optically Normal Galaxies (XBONG, Comastri et al. 2002), Extremely Red Objects (e.g. Brusa et al. 2005), Sub Millimeter Galaxies (e.g. Alexander et al. 2005) high- z starforming systems (e.g. F, Fiore et al. 2008). In many of these cases, the AGN responsible for the X-ray emission is overwhelmed at longer wavelength by the host galaxy light and/or the obscuration might be connected to processes within the host galaxy itself, such as the star formation rate and the presence of dust lanes or starburst disks (see e.g. Hopkins et al. 2009). This suggests that the accretion activity (especially in high-redshift sources) is unambiguously revealed thanks to the presence of a strong X-ray emission (see e.g. discussion in Brusa et al. 2009a) and therefore, the combination of both X-ray and optical classifications can be crucial to fully assess the nature of the candidate AGN.

The high level of completeness in redshift determination for a large number of X-ray selected AGN (up to a few thousands) has made possible a robust determination of the luminosity function and evolution of unobscured and mildly obscured AGN which turned out to be luminosity dependent: the space density of bright QSOs ($L_X > 10^{44}$ erg s⁻¹) peaks at $z \sim 2-3$, to be compared with the $z \sim 0.7-1$ peak of lower luminosity Seyfert galaxies (Ueda et al. 2003, La Franca et al. 2005, Silverman et al. 2008a, Ebrero et al. 2009). Based on these works, Marconi et al. (2004) and Merloni (2004) were the first to pro-

pose that SMBH undergo a “anti-hierarchical” evolution, in the form a differential growth (earlier and faster for larger black holes). This anti-hierarchical behavior observed in AGN evolution (similar to that observed in normal galaxies, e.g. Cowie et al. 1996) provided an important, independent, confirmation that the formation and evolution of SMBH and their host galaxies are likely different aspects of the same astrophysical problem. In particular, the accretion onto supermassive Black Holes triggered by galaxies mergers and/or collisions may provide the “feedback” needed in almost all recent models for galaxies formation and evolution, in order to recover the properties (masses, luminosity, clustering) we observe today in local systems.

In this general framework the differences between “obscured” and “unobscured” AGN are no longer and uniquely described under a zeroth-order geometrical unification model (in which they are simply related to orientation effects, Antonucci & Miller 1985), but can be interpreted as due to the fact that the *same* object is observed in *different evolutive* phases. This hypothesis is further supported by the finding that absorption is much more common at low luminosities (Ueda et al. 2003, Maiolino et al. 2007) and at high redshift (La Franca et al. 2005, Treister & Urry 2006, Hasinger 2008) as emerges mainly from X-ray surveys. The luminosity and redshift dependence of the obscuring fraction may be naturally linked to the AGN radiative power (related to the intrinsic X-ray luminosity) which is able to ionize and expel gas and dust (more common at high- z) from the nuclear regions, nicely fitting the current framework of AGN formation and evolution sketched above (see, for example, Hopkins et al. 2006 and this volume).

The complete picture is likely to be much more complicated, depending on many other parameters (such as, e.g., the BH mass, the Eddington ratio, the QSO duty cycle), and in particular related to the complex “lightcurves” of AGN, which, in turns, depend on the detailed hydrodynamics adopted in the simulations. A correct and complete identification of unobscured, obscured and highly obscured AGN at all redshifts (and especially in the $z=1-3$ interval, where most of the feedback is expected to happen) is therefore crucial for a comprehensive understanding of the still little explored phase of the common growth of SMBHs and their host galaxies.

Here I highlight recent results the characterization of the high luminosity tail of the X-ray luminosity function from the COSMOS survey, and on the host galaxy properties of obscured AGN at cosmological distance, from an analysis of X-ray selected sources in the Chandra Deep Field South (CDFS). I also present evidence for an evolution of the $M_{BH}-M_{Bulge}$ relation as derived from optically selected BL AGN from the zCOSMOS survey (almost all of them also X-ray emitters).

1. The high-luminosity tail of X-ray selected AGN: results from the COSMOS survey

The high completeness in optical identifications of the XMM-COSMOS sample (Brusa et al. 2009b) and the availability of spectroscopic and photometric redshifts (Salvato et al. 2009) allows us to estimate the number densities of AGNs as a function of luminosity and redshift. In calculating the binned number density evolution we considered only the subsample of sources detected in the hard (2-10 keV) band, and included in the flux limited sample (925 sources at $S_x = 6 \times 10^{-15}$ erg s $^{-1}$ cm $^{-2}$; $\sim 60\%$ with spectroscopic redshifts available). Since the hardness ratios between the hard and soft bands give the estimates of the absorption column density, we present the XLF of the de-absorbed 2-10 keV luminosity. In our first analysis, we use the traditional $\sum 1/V_a$ estimator (Avni & Bahcall 1980). Additional details on the method used in deriving the XLF are given in Brusa et al. (2010) and Miyaji et al. (in preparation).

We compared our first estimates of the number density evolution of the most luminous AGN population with recent measurements. The results are presented in Figure 1, where the number density of XMM-COSMOS sources is plotted versus the redshift in the luminosity bin $\text{Log}L_X = 44.5 - 47$ (squares). We only included the bins where the lowest L_X lowest z boundary corresponds to a 2-10 keV flux above our limit for plotting. In the same figure we plot the data points obtained from the AEGIS survey by Aird et al. (2010); circles), along with their best fit luminosity function (black curve). The results based on 6 datapoints within $z=1-3$, with ~ 20 objects each may provide robust constraints on the shape of the XLF. In particular, the XMM-COSMOS data points seem to favour a higher redshift ($z \sim 2$) peak for the space density of luminous quasars as predicted by a LDDE parameterization, represented in the figure by the Ebrero et al. (2009, short-dashed curve) and the Silverman et al. (2008, long-dashed curve) luminosity functions, though different in the details, and reproduced by XRB synthesis models (Gilli, Comastri & Hasinger 2007; dot-dashed curve) rather than the lower redshift ($z \sim 1$) peak expected from LADE model recently proposed by Aird et al. (2010).

2. Black Hole and Star formation activity at $z > 1$

In order to study the host-galaxies of obscured AGN, we defined a sample of 116 “bona fide” obscured AGN, detected in the 1Ms CDFS observation (Alexander et al. 2003) and for which deep Infrared (IRAC and MIPS), K-band and multiwavelength optical photometry is available (from Grazian et al. 2006, the MUSIC survey) We selected sources without broad lines in the optical spectra and with small optical nuclear emission with respect to the host galaxy optical emission.

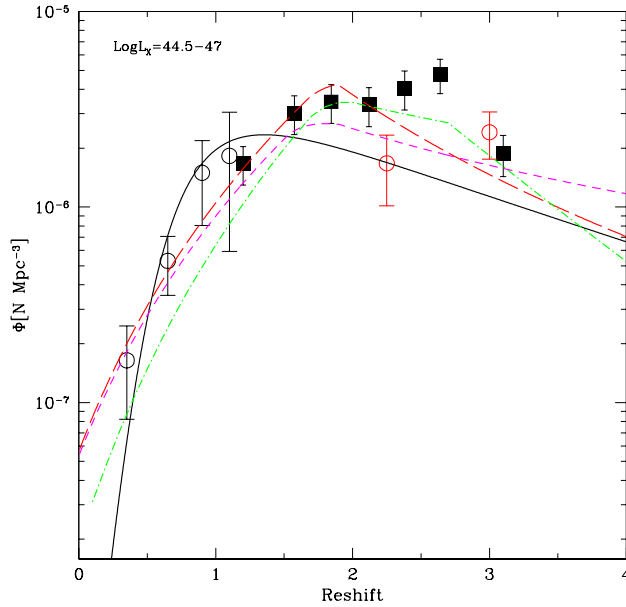


Figure 1. The number density evolution from the XMM-COSMOS 53 field AGN (squares) compared with recent results from Aird et al. (2010; circles, and black solid line), Ebrero et al. (2009; short-dashed curve), Silverman et al. (2008; long-dashed curve), and the expectation of XRB synthesis models taken from Gilli et al. (2007, dot-dashed curve).

We found that the hosts of obscured AGN are redder in (U-V) rest frame than the overall galaxy population at the same redshift: in particular, obscured AGN mainly populate the red sequence and the green valley in the color-magnitude plots in agreement with the results of Silverman et al. (2008b). For the MUSIC sample the U-V galaxy colors are strongly correlated with the K band absolute magnitude (Figure 2), and therefore with the galaxy stellar mass, with the most massive systems having a redder color. The hosts of the obscured AGN are therefore found in the red-massive tail of the distribution of optically selected galaxies in all three redshift bins considered (see labels in the figure). AGN feedback is often invoked as one of the main responsible for the observed galaxy colors (e.g. Nandra et al. 2007, Hasinger 2008). However, it is well known that the main ingredient for nuclear activity is the presence of a SMBH in galaxy nuclei, and that SMBHs are found nearly exclusively in massive galaxies (e.g. Magorrian et al. 1998). Therefore, it is not truly surprising to find AGN hosted in massive galaxies and the simple presence of AGN in massive red galaxies is not enough to argue for a significant feedback effect on the observed colors, because of the strong color-mass correlation. Were AGN feedback responsible for the observed red colors, since galaxy colors are strongly correlated with the galaxy mass and AGN are found preferably in massive galaxies, then AGN feedback should be also considered as one of the main players in the building of the galaxy mass-color correlation.

We found that about 2/3 of the obscured AGN hosts at all redshifts show substantial ($> 10 M_{\odot} \text{ yr}^{-1}$) star formation activity (Figure 3, where two histograms of the SFR derived from SED fitting are reported, for optical and Infrared selected samples) and

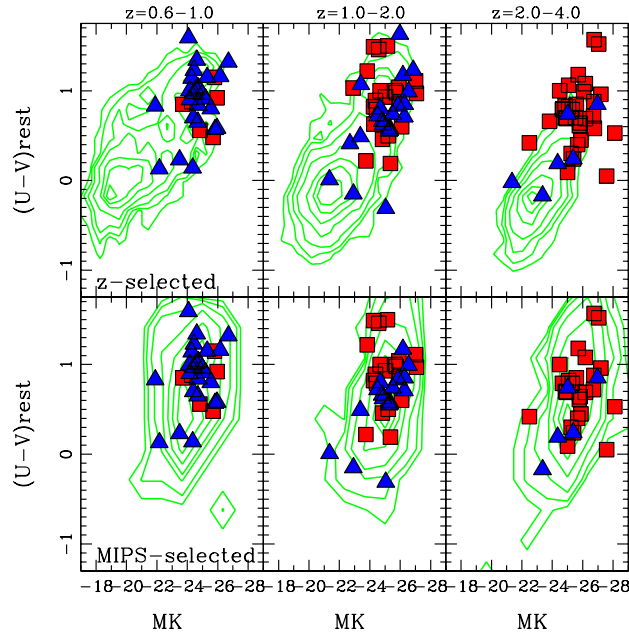


Figure 2. U-V(rest frame) vs. the absolute K-band magnitude for the obscured AGN (squares and triangles) and the underlying galaxy population (contours). The upper panels show the comparison of the X-ray selected sources with the optically-selected (z-band) galaxy population in three different redshift bins: $z=0.6-1.0$, $z=1-2$, and $z=2.4$ from left to right, respectively. The lower panels show the comparison for the subsample of objects detected also at 24 micron, in the same redshift bins.

about half live in galaxies which are still actively forming stars with respect to their mass. For these sources, the observed red colors are likely due to dust extinction rather than evolved stellar population. We then conclude that a significant fraction of obscured AGN live in massive, dusty star-forming galaxies with red optical colors.

We compared the number of obscured AGN and of all X-ray selected AGN to the number of field galaxies in broad bins of galaxy stellar mass ($M_* = 10^{10} - 10^{12} M_\odot$) and redshifts ($z=0.6-1$, $z=1-2$, $z=2-4$). We find that the AGN fraction increases with the host galaxy stellar mass, from $\sim 1\%$ at $M_* \sim 10^{10} M_\odot$ to $\sim 30\%$ at $M_* \sim 3 \times 10^{11} M_\odot$ (see also Yamada et al. 2009), and the actual trend of increasing AGN fraction as a function of the stellar mass is probably steeper given the incompleteness of the MUSIC sample at $M_* < 10^{11} M_\odot$ (see Figure 4). We compared this trend with that observed in the local Universe (Best et al. 2005) for AGN with luminosity above similar thresholds. While the observed trend is the same, in all the investigated redshift bins the AGN fraction is higher than that observed in the local Universe, and it could likely be even higher. In fact, we are comparing here AGN selected with two different methods: forbidden emission line luminosity (SDSS) and X-ray emission (GOODS). The latter sample does not contain most Compton thick AGN. On the other hand, Compton thick AGN may well be present in [OIII] selected AGN samples. The fraction of Compton thick AGN not directly detected in deep Chandra surveys is estimated between 40% and 100% of the X-ray selected AGN, using infrared selection or other techniques (see Donley et al. 2008, Fiore et al. 2008 and references therein). Therefore, under the simplest assumption that this Compton Thick AGN fraction is constant with the galaxy mass, the discrepancy observed in Figure 10 can increase by up of a factor of 2.

The fraction of active galaxies to the total galaxy population is proportional to the AGN duty cycle. Our results would thus suggest higher AGN duty cycles at $z=2-4$ than at

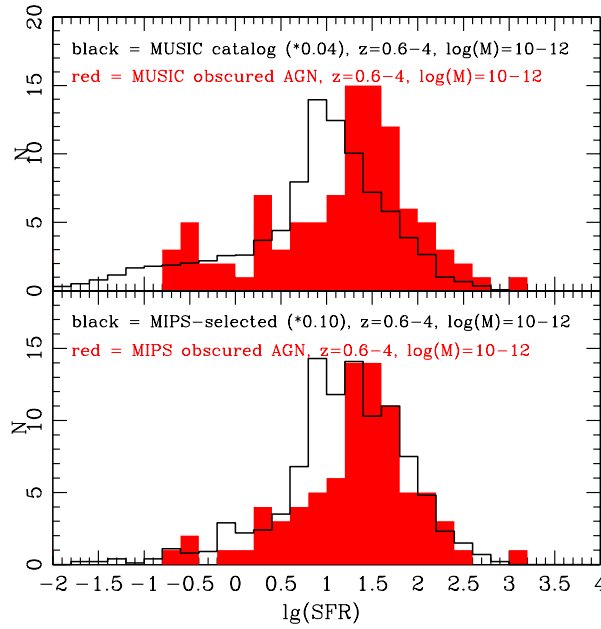


Figure 3. The distribution of the SFR for both the optically (upper) and MIPS (lower) selected sample of field galaxies (open histogram) and obscured AGN (filled histogram) in the redshift interval $z=1-4$ and in a specific stellar mass range ($M_* = 10^{10} - 10^{12} M_\odot$).

$z=0$, in agreement with expectations from most recent semi-analytic models (e.g. ?), in which at higher redshift the AGN activity is present in a larger number of galaxies than locally.

The fact that the most luminous obscured AGN are found in the most massive galaxies at all investigated redshifts may suggest that the L/L_{Edd} of the obscured AGN is similar, particularly in the case of the most luminous sources ($\log L_X > 43 \text{ erg s}^{-1}$), for which the threshold in luminosity introduces a bias against the sources accreting at lower rates in the lowest redshift bin. Assuming the local Magorrian relation between M_{BH} and M_* (e.g. Marconi & Hunt 2003) and a bolometric correction of 20 (e.g. Marconi et al. 2004) the median observed values of L_X/M_* correspond to $L/L_{Edd} \sim 0.1$. Although suffering from large uncertainties associated with the stellar mass and BH mass estimates, this value can be considered as representative of the accretion state of the most luminous, obscured AGN in the present sample. Similar results are obtained for Chandra Deep Field North X-ray sources at $z=2-4$ (Yamada et al. 2009) and are also typical of unobscured Type 1 AGN at $z > 1$ (see Merloni et al. 2009).

3. The evolution of M_{BH} - M_{Bulge} relation

Local scaling relations have proved themselves unable to unambiguously determine the physical nature of the SMBH-galaxy coupling. A large number of theoretical models for the AGN-galaxy interaction have been proposed, all tuned to reproduce the $z=0$ observations. One obvious way out of this impasse is the study of the scaling relations' evolution, which had, until recently, been limited to a handful of objects in narrow redshift windows

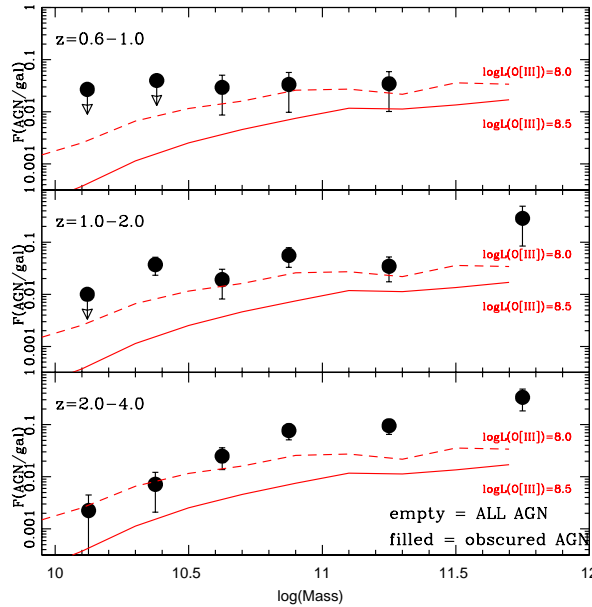


Figure 4. Fraction of obscured AGN with $L_X > 10^{43} \text{ erg s}^{-1}$ as a function of the stellar mass in three different redshift bins. Filled circles refer to the “obsured” AGN sample. The dashed (continuous) lines represent the fraction of AGN with $L(OIII) > 10^{8.0}$ ($10^{8.5}$) L_\odot in an optically selected sample in the local Universe ($z < 0.2$) from the SDSS (Best et al. 2005).

(Peng et al. 2006, & this volume; Woo et al. 2008 & this volume, Jahnke et al. 2009 & this volume).

Within the zCOSMOS collaboration (a massive spectroscopic campaigns with $\sim 10,000$ spectra of galaxies and AGN, Lilly et al. 2007), we have pioneered a new method to unveil the intrinsic physical properties of AGN hosts, using the unprecedented multi-wavelength coverage of the COSMOS field. In Merloni et al. (2009), we have been able to measure rest frame K-band luminosities and total stellar masses, M_* , of the hosts of 89 broad-line (un-obscured) AGN in the redshift range $1 < z < 2.2$, for which we measured the black hole mass, M_{BH} , through the virial method (see e.g. Peterson et al. 2004 & this volume). This sample constitutes the largest high redshift sample so far for which reliable black hole and galaxy masses are available. We found that, as compared to the local value, the average black hole to host galaxy mass ratio appears to evolve positively with redshift, with a best fit evolution of the form $(1+z)^{0.68 \pm 0.12}$ (see Figure 5). A thorough analysis of observational biases induced by intrinsic scatter in the scaling relations reinforces the conclusion that an evolution of the $M_{BH} - M_*$ relation must ensue for actively growing black holes at early times: either its overall normalization, or its intrinsic scatter (or both) appear to increase with redshift.

Acknowledgements

It is a pleasure to acknowledge the contribution of Takamitsu Miyaji, Andrea Comastri, Fabrizio Fiore, Andrea Merloni & Angela Bongiorno in obtaining the results I presented

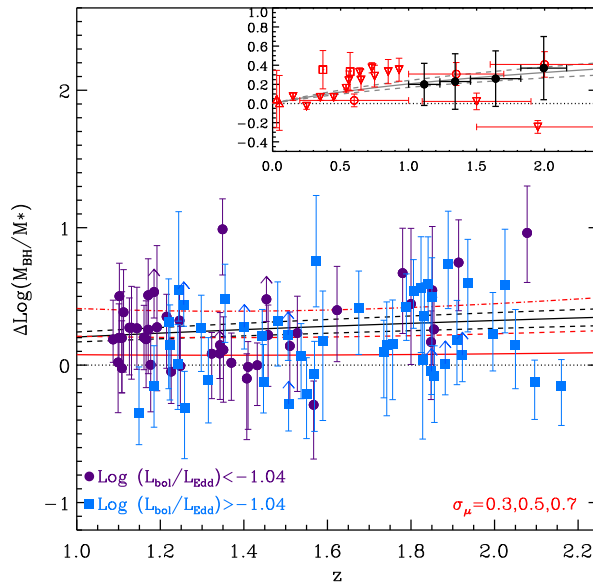


Figure 5. Redshift evolution of the offset measured for zCOSMOS type 1 AGN from the local $M_{BH}-M_*$ relation. Different symbols identify different ranges of Eddington ratios with upwards arrows representing upper limit on the host galaxy mass. The solid black line shows the best fit obtained assuming an evolution of the form $\Delta\text{Log}(M_{BH}/M_*)(z) = \delta(1+z)$ with $\delta = 0.68 \pm 0.12$. The solid, dashed and dot-dashed lines show the bias due to an intrinsic scatter in the scaling relation of 0.3, 0.5 and 0.7 dex, respectively. In the inset we show a comparison of our data (black circles, binned) with data collected from the literature.

at the conference, along with the efforts of many people from the XMM-COSMOS, zCOSMOS and CDFS/MUSIC collaborations. Many thanks to the organizers of the meeting, and in particular Bradley Peterson, for offering me the possibility to attend this great symposium.

References

- Aird, J., Nandra, K., Laird, E.S., et al., 2010, *MNRAS*,
 Alexander, D.M., Bauer, F.E., Brandt, W.N., et al. 2003, *AJ*, 126, 539
 Alexander, D.M., Bauer, F.E., Chapman, S.C. et al. 2005, *ApJ*, 632, 736
 Antonucci, R.R. & Miller, J.S., 1985, *ApJ*, 297, 621
 Avni Y., Bahcall J.N. 1980, *ApJ* 235, 694
 Best, P.N., Kauffmann, G., Heckman, T.M., Brinchmann, J., Charlot, S., Ivezić, Z., White, S.D.M., 2005, *MNRAS*, 362, 35
 Brandt, N.W. & Hasinger, G. 2005, *ARAA*, 43, 827
 Brusa, M., Comastri, A., Daddi, E., et al. 2005, *A&A*, 432, 69
 Brusa, M., Fiore, F., et al., 2009, *A&A*, 507, 1277
 Brusa, M., Comastri, A., Gilli, R., et al., 2009, *ApJ*, 693, 8
 Brusa, M., Civano, F., Comastri, A., et al., 2010, *ApJ*, in press, arXiv:1004.2790
 Comastri, A., Mignoli, M., Ciliegi, P., et al. 2002, *ApJL*, 571, 771
 Cowie, L.L., Songaila, A., Hu, E.M., Cohen, J.G., 1996, *AJ*, 112, 839
 Daddi, E., Dickinson, M., Morrison, G., et al. 2007 *ApJ* 670, 156
 Donley, J.L., Rieke, G.H., Perez-Gonzalez, P.G., Barro, G., *ApJ*, 687, 111
 Ebrero, J., et al. 2009, *A&A*, 493, 55
 Fiore, F., Grazian A., Santini P., et al. 2008, *ApJ*, 692, 74
 Gilli, R., Comastri, A., & Hasinger, G. 2007, *A&A*, 463, 79
 Grazian A., Fontana, A., de Santis, C. et al. 2006, *A&A*, 449, 951
 Hasinger, G. 2008, *A&A*, 490, 905
 Hickox, R., 2009, *Chandra Newsletter cover article*, arXiv:0904.3543
 Hopkins, P.F., Hernquist, L. Cox, T.J., Di Matteo, T., Robertson, B., Springel, V., 2006, *ApJS*, 163, 1
 Hopkins, P. F., Hickox, R., Quataert, E., & Hernquist, L. 2009, *MNRAS*, 398, 333
 Jahnke, K., Bongiorno, A., Brusa, M., et al. 2009, *ApJL*, 706, 215
 La Franca F., Fiore F., Comastri A., et al., 2005, *ApJ*, 635, 864
 Lilly, S.J., Le Fèvre, O., Renzini, A., et al., 2007, *ApJS*, 172, 70
 Magorrian, J., et al., 1998, *AJ*, 115, 2285
 Maiolino, R., et al. 2007, *A&A*
 Marconi, A., & Hunt, L.K., 2003, *ApJ*, 589, L21
 Marconi, A., Risaliti, G., Gilli, R., Hunt, L.K., Maiolino, R., & Salvati, M., 2004, *MNRAS*, 351, 169
 Menci N., Fiore, F., Puccetti, S. Cavaliere, A. 2008, *ApJ*, 686, 219
 Merloni, A., 2004, *MNRAS*, 353, 1035
 Merloni, A., Bongiorno A., et al., 2009, *ApJ*, 708, 38
 Peng, C.Y., et al., 2006, *ApJ*, 649, 616
 Peterson, B. M., Ferrarese, L., Gilbert, K.M., et al. 2004, *ApJ*, 613, 682
 Salvato, M., Hasinger, G., Ilbert, O., et al., 2009, *ApJ*, 690, 1250
 Silverman, J.D., Green, P.J., Barkhouse, W.A., et al., 2008, *ApJ*, 679, 118
 Silverman, J.D., Mainieri, V., Lehmer, B., et al., 2008, *ApJ*, 675, 1025
 Treister, E., & Urry, C.M., 2006, *ApJL* 652, 79
 Ueda, Y., Akiyama, M., Ohta, K., & Miyaji, T., 2003, *ApJ* 598, 886
 Yamada, T., Kajisawa, M., Akiyama, M., et al., 2009, *ApJ*, 699, 1354
 Woo, J.H., Treu, T., Malkan, M.A., Blandford, R.D., 2008, *ApJ*, 681, 925